11 May 2026

Electrochemical Synthesis of Slaked Lime Utilizing a Diaphragm Flow Cell

J. Gage Wright[1], Jason W. Misleh[1], Nawal M. Alghoraibi[1], Matthew W. Kanan[1]

1. Department of Chemistry, Stanford University

Abstract

Slaked lime ($Ca(OH)_2$) is one of the most widely utilized chemicals, with applications in diverse industries including construction, mining, water treatment, and chemical manufacturing. Currently, $Ca(OH)_2$ is synthesized by coal-fired calcination of ($CaCO_3$) to make CaO, followed by an exothermic hydration. Converting $CaCO_3$ into $Ca(OH)_2$ using electrochemically generated acid and base has attracted great interest because it could be powered by renewable electricity and would generate the CO_2 byproduct in a pure form. Previous electrochemical $Ca(OH)_2$ syntheses have incorporated the processing of calcium salts within the electrochemical cell to avoid acid-base recombination losses, but these cells have poor stability and high energy demand. Herein we show that production of high-salinity acid and base solutions using a diaphragm flow cell (DFC) coupled with ex situ processing of $CaCO_3$ substantially improves the efficiency of electrochemical $Ca(OH)_2$ production. Using a closed loop with a simple KCl salt solution, we demonstrate the synthesis of > 99% pure $Ca(OH)_2$ for 0.088 to 0.10 kWh per mole at productive current densities of 158 to 334 mA cm^{-2}.

Keywords

Electrochemistry, Slaked lime, Cement, Clinker, Electrolysis, Acid Base, Decarbonization, Calcium, Limestone, Hydrometallurgy, Salt splitting

Electrochemical Synthesis of Slaked Lime Utilizing a Diaphragm Flow Cell

J. Gage Wright, Jason W. Misleh, Nawal M. Alghoraibi, and Matthew W. Kanan*

Department of Chemistry, Stanford University, Stanford, California 94305, USA

*Corresponding Author. Email: mkanan@stanford.edu

Abstract

Slaked lime ($Ca(OH)_2$) is one of the most widely utilized chemicals, with applications in diverse industries including construction, mining, water treatment, and chemical manufacturing. Currently, $Ca(OH)_2$ is synthesized by coal-fired calcination of ($CaCO_3$) to make CaO, followed by an exothermic hydration. Converting $CaCO_3$ into $Ca(OH)_2$ using electrochemically generated acid and base has attracted great interest because it could be powered by renewable electricity and would generate the CO_2 byproduct in a pure form. Previous electrochemical $Ca(OH)_2$ syntheses have incorporated the processing of calcium salts within the electrochemical cell to avoid acid-base recombination losses, but these cells have poor stability and high energy demand. Herein we show that production of high-salinity acid and base solutions using a diaphragm flow cell (DFC) coupled with ex situ processing of $CaCO_3$ substantially improves the efficiency of electrochemical $Ca(OH)_2$ production. Using a closed loop with a simple KCl salt solution, we demonstrate the synthesis of $> 99\%$ pure $Ca(OH)_2$ for 0.088 to 0.10 kWh per mole at productive current densities of 158 to 334 mA cm^{-2}.

Introduction

Solid bases are utilized on an enormous scale across several major industries. With more than 400 Mt produced annually, quicklime (CaO) is the dominant solid base and the largest chemical product by volume, substantially exceeding the scale of organic commodities like ethylene and propylene.[1] Approximately half of the CaO produced is converted to slaked lime ($Ca(OH)_2$) to increase its reactivity for low-temperature applications like water treatment, desulfurization, and various processes in the food and chemical industries.[2–4] Slaked lime is the preferred base for many applications because of its low cost and the low solubility

of calcium salts (e.g., $CaSO_4$, $CaCO_3$), which allows for easy separation and removal of calcium byproducts after the base is consumed. Due to its high reactivity and ability to be regenerated, slaked lime is also used in direct air capture processes, either as the sorbent itself or as a sorbent regenerant.[5,6]

The feedstock for CaO and $Ca(OH)_2$ is limestone, a rock rich in calcite ($CaCO_3$), which is Earth's most abundant and concentrated calcium resource.[7] To make CaO, limestone is calcined at > 900 °C in kilns using fossil fuel, typically coal, to provide the energy for the endothermic reaction (Equation 1). Calcination requires an average of 0.070 kWh of thermal energy per mol of CaO and emits ~1.14 tons of CO_2 per ton of CaO according to the European Lime Association, with some variation for both of these values depending on the type of kiln.[4] The reaction of CaO and H_2O to make $Ca(OH)_2$ is exothermic (Equation 2) and typically operates with minimal process energy demand. Nonetheless, the production of CaO as an intermediate for $Ca(OH)_2$ necessitates a minimum of 57% more thermal energy than the enthalpic requirement for the net reaction from $CaCO_3$ (Equation 3), providing an opportunity for efficiency gains by accessing $Ca(OH)_2$ directly.

$$\mathrm{CaCO_3} \longrightarrow \mathrm{CaO + CO_2} \qquad \Delta H^\circ = 178 \text{ kJ/mol} \tag{1}$$

$$\mathrm{CaO + H_2O} \longrightarrow \mathrm{Ca(OH)_2} \qquad \Delta H^\circ = -65 \text{ kJ/mol} \tag{2}$$

$$\mathrm{CaCO_3 + H_2O} \longrightarrow \mathrm{Ca(OH)_2 + CO_2} \qquad \Delta H^\circ = 113 \text{ kJ/mol} \tag{3}$$

As an alternative to calcination and hydration, $Ca(OH)_2$ can be produced from limestone by sequential application of aqueous acid and base (Equations 4 and 5). Regeneration of the acid and base by electrochemical salt splitting (Equation 6) offers a low-temperature, electrically-powered version of slaked lime production.[8–15] This approach offers the added benefit of evolving the stoichiometric equivalent of CO_2 in much higher purity, without any of the contaminants found in lime kiln off-gas (NO_x, SO_x, O_2, CO, etc.), which greatly simplifies its sequestration or industrial use. By using low-carbon electricity to power electrochemical acid and base production and sequestering the CO_2 from $CaCO_3$ acidification, it is possible to produce $Ca(OH)_2$ with near-zero emissions. It could also be of interest to use $Ca(OH)_2$ produced through this process as a feedstock for CaO, inverting the current sequence, since $Ca(OH)_2$ dehydration to CaO can be achieved using less heat (Equation 2) at a lower temperature (~500 °C).[8,9] Thus, zero-emission $Ca(OH)_2$ could provide a path to decarbonize CaO and products derived from it, including steel and cement. More broadly, an acid-base approach can be applied to produce $Ca(OH)_2$ from other calcium resources like silicates, avoiding stoichiometric CO_2 altogether.[15–18]

$$\mathrm{CaCO_3 + 2\,HX} \longrightarrow \mathrm{CaX_2 + H_2O + CO_2} \tag{4}$$

$$\mathrm{CaX_2 + 2\,MOH} \longrightarrow \mathrm{Ca(OH)_2 + 2\,MX} \tag{5}$$

$$\mathrm{2\,MX + 2\,H_2O} \longrightarrow \mathrm{2\,MOH + 2\,HX} \tag{6}$$

Commercial bipolar membrane electrodialysis (BPMED) technology generates relatively concentrated (> 1 M) acid and base solutions by electrochemical salt splitting. Although BPMED could in principle be used for closed-loop electrochemical $Ca(OH)_2$ synthesis, these systems suffer from high energy demands and low productive current densities (< 50 mA cm^{-2}) associated with the reliance on multiple ion exchange membranes (IEMs) to control ion transport. Here, productive current density (j_{prod}) means the current density resulting in separated acid and base ions exiting the cell. Several research groups have described electrochemical $Ca(OH)_2$ synthesis using systems that dissolve $CaCO_3$ or precipitate $Ca(OH)_2$ in the cell as a strategy to prevent acid-base recombination.[10,12,13] Some of these systems can reach j_{prod} > 100 mA cm^{-2}, but processing solids within the cell has prevented stable operation and imposes a high energy cost from additional resistive losses (see below for more detailed discussion).

We have recently reported diaphragm flow cells (DFCs) that can produce concentrated (> 1 M) acid and base using a simple porous diaphragm separator instead of IEMs. The DFC uses the transport of supporting electrolyte ions to suppress H^+/OH^- recombination, which supports much higher j_{prod} (hundreds of mA cm^{-2}) with significantly reduced energy demand compared to BPMED systems.[19–21] In this study, we investigate electrochemical $Ca(OH)_2$ synthesis utilizing the DFC to generate acid and base in a closed loop process consisting of acid and base generation, Ca^{2+} leaching, precipitation, and electrolyte recovery (Figure 1). By balancing the competing factors that affect acid-base production and product precipitation, we demonstrate the production > 99% pure $Ca(OH)_2$ with an energy demand of 0.088 kWh per mol $Ca(OH)_2$ at j_{prod} of 158 mA cm^{-2} and 0.10 kWh per mol at 334 mA cm^{-2}.

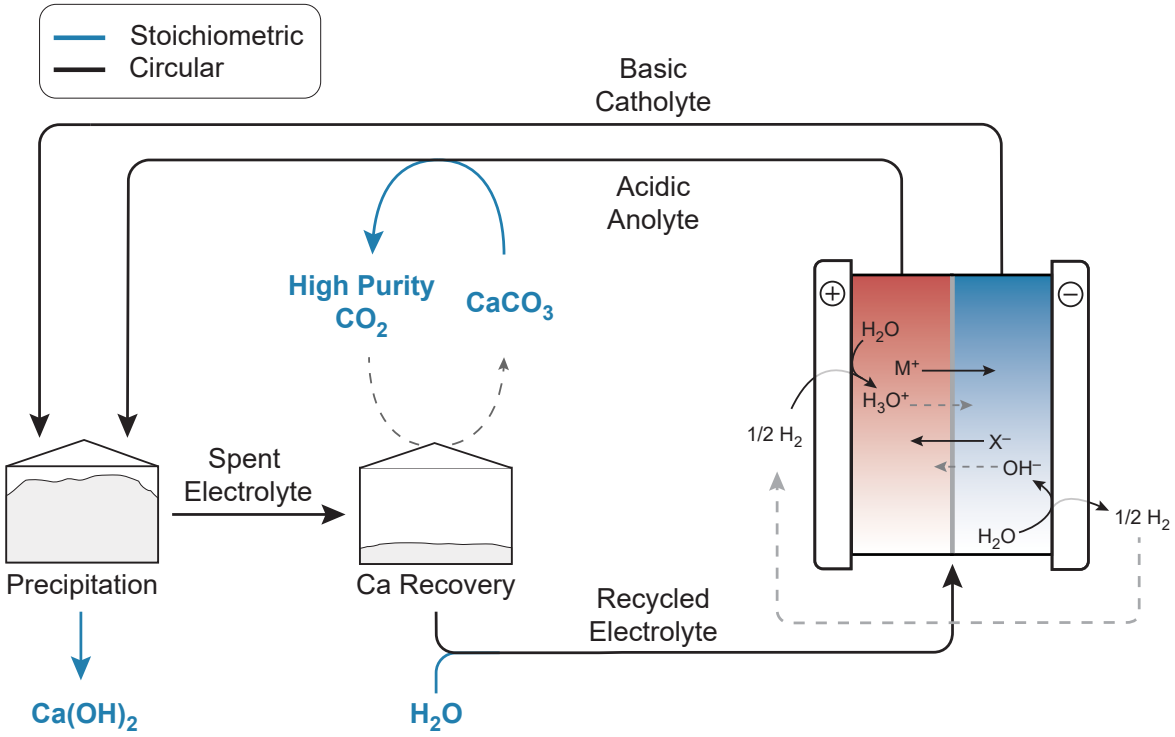

Figure 1: Process concept for the transformation of $CaCO_3$ into $Ca(OH)_2$. Acid and base are first produced electrochemically in the Diaphragm Flow Cell. The acid is used to dissolve $CaCO_3$, producing high purity CO_2 and Ca^{2+}-rich electrolyte, which is then combined with the base to precipitate $Ca(OH)_2$. Residual Ca^{2+} is recovered as $CaCO_3$ using some of the CO_2 liberated during the dissolution step.

Results and Discussion

The design of the DFC is described in detail in our previous work.[20] Briefly, it consists of two electrolyte compartments supported by woven mesh spacers and separated by a non-selective, porous diaphragm. As electrolyte is pumped through the cell compartments, H^+ and OH^- are generated at the anode and cathode by gas diffusion electrodes that perform the hydrogen oxidation and hydrogen evolution reactions, resulting in acidic and alkaline outputs (Figure 1). The energy demand per mol of acid and base generated by the cell (E_{ab}) is given by Equation 7, where E_{cell} is the full cell voltage, CE is the current efficiency, and F is the Faraday constant. CE reflects the competition between current carried by the supporting electrolyte ions versus current carried by H^+ and/or OH^- crossover that results in recombination losses (100% CE corresponds to no recombination losses). The output concentration (c_{output}) of the acid and/or base stream depends on the total current density (j_{tot}), CE, and the electrode area-normalized flow rate (Q) as shown in Equation 8, where

j_{prod} is j_{tot} multiplied by CE.

$$E_{ab} = \frac{E_{cell}F}{\text{CE}} \tag{7}$$

$$c_{output} = \frac{j_{tot} \cdot \text{CE}}{QF} = \frac{j_{prod}}{QF} \tag{8}$$

The yield of $Ca(OH)_2$ precipitation with our approach has a strong dependence on c_{output} of both the acid and base streams because of the non-negligible solubility of $Ca(OH)_2$ (see below). With this constraint in mind, we focused our studies on two electrolytes: 3 M KCl and a mixed electrolyte consisting of 2.5 M KCl with 0.5 M potassium formate ($KHCO_2$). Both electrolytes have relatively high conductivity (we measured a conductivity of 328 mS cm^{-1} for 3 M KCl), which reduces iR losses, and both $CaCl_2$ and $Ca(HCO_2)_2$ are soluble in water at concentrations > 1 M. Replacing 0.5 M chloride with formate provides a significant buffer capacity that "masks" H^+ as neutral formic acid, which is still acidic enough to easily dissolve $CaCO_3$. While sulfate is also an effective H^+ mask,[19] it cannot be used for $Ca(OH)_2$ production because it leads to rapid precipitation of $CaSO_4$. The cell temperature was maintained at 50 °C for all measurements, since the steady-state temperature of a large scale stack is likely 50 – 70 °C.[20]

We performed electrolysis experiments over a j_{tot} range of 100 – 400 mA cm^{-2}, measuring E_{cell} and CE every 100 mA cm^{-2} while varying the flow rate appropriately to maintain one of three $j_{tot}(QF)^{-1}$ ratios (Figure 2 and Table S1). The same flow rate was used for both compartments. The $j_{tot}(QF)^{-1}$ ratio has units of concentration and represents what the output concentration of acid and base would be if there were no recombination losses. As seen in Figure 2A and D, CE increases monotonically with j_{tot} for both electrolytes. This effect can be explained by the relative contributions of ion diffusion and electromigration and their dependence on j_{tot}. As j_{tot} is increased, diffusive ion transport, which consists mostly of H^+ and OH^-, becomes dominated by electromigration, which consists mostly of the supporting electrolyte.[20] However, for a given j_{tot}, higher values of $j_{tot}(QF)^{-1}$ (i.e., lower Q) increase the driving forces for product crossover and recombination, leading to decreased CE. Nonetheless, the results in Figure 2A and D demonstrate the ability of the DFC to generate concentrated acid and base with high CE (75 – 85%) at industrially relevant current densities of 200 – 400 mA cm^{-2}.

The use of the mixed 0.5 M $KHCO_2$ + 2.5 M KCl electrolyte resulted in higher CE than seen with 3 M KCl, which is consistent with reduction of H^+ crossover by masking as formic acid. However, the improved CE was partially offset by a somewhat higher E_{cell} for the mixed electrolyte compared to 3 M KCl (Figure 2B, E), which arises from the reduced concentration of H^+ and the lower molar conductivity of formate compared to chloride. Interestingly, the lowest cell potentials were achieved at the intermediate $j_{tot}(QF)^{-1}$ ratio. Increasing the concentrations of H^+ and OH^- increases the bulk conductivity, which reduces resistive losses, but also increases the open circuit potential and concentration overpotential. The offsetting differences in CE and E_{cell} resulted in similar overall energy demand for acid-base production (E_{ab}) with 3 M KCl vs. 0.5 M $KHCO_2$ + 2.5 M KCl (Figure 2C, F).

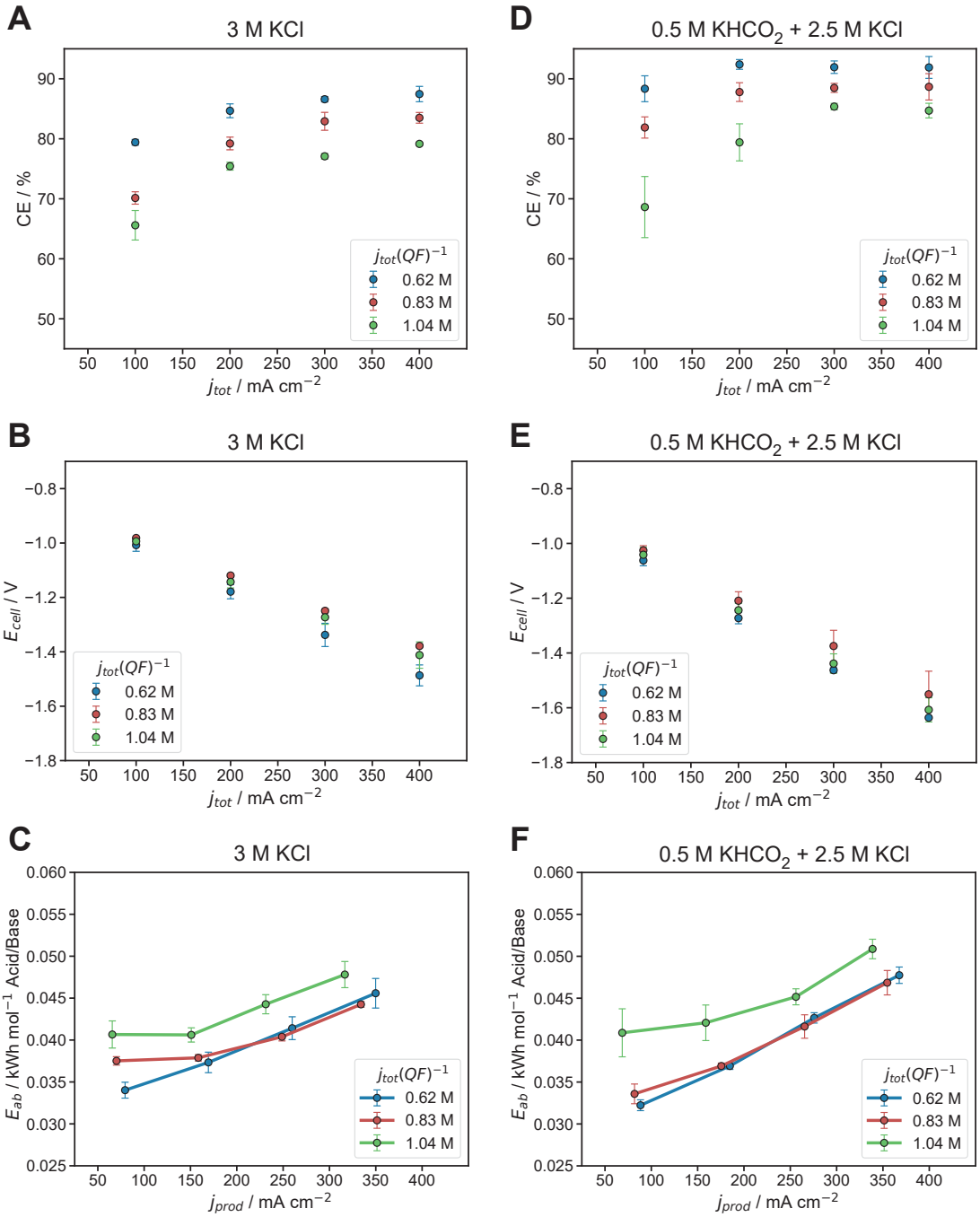

Figure 2: Cell performance at 50 °C as a function of current density for different sets of flow rates such that the production $j_{tot}(QF)^{-1}$ remains constant. A) Current efficiencies and B) cell potentials for 3 M KCl versus total current density. C) Energy required per mole to generate acid and base using 3 M KCl electrolyte vs. productive current density. D) Current efficiencies and E) cell potentials for 0.5 M $KHCO_2$ + 2.5 M KCl versus total current density. F) Energy required per mole to generate acid and base using 0.5 M $KHCO_2$ + 2.5 M KCl electrolyte vs. productive current density. Error bars represent the standard deviation of at least 3 independent samples.

A key challenge for electrochemical $Ca(OH)_2$ production using our ex situ processing approach is achieving high precipitation efficiency (PE). Other works have shown that $Ca(OH)_2$ can be precipitated with very high efficiency either by dissolving limestone slurries in the acid compartment to concentrate Ca^{2+} or by using a high concentration Ca^{2+} stream to precipitate $Ca(OH)_2$ within the cell, but at the cost of stability and/or extremely high E_{cell}.[8,10,13] Our strategy seeks to avoid these problems by performing processing outside of the cell with concentrated acid and base outputs. In this case, the PE depends on the difference between the calcium loading (L) and the solubility of $Ca(OH)_2$ (S) according to Equation 9, where the loading is the nominal concentration of dissolved Ca^{2+} in the total volume of the combined streams (i.e. immediately after combining the output streams but before precipitation of $Ca(OH)_2$ occurs). The loading depends on the flow rates and output concentrations of the DFC according to Equation 10, where Q_a and Q_c are the electrode area-normalized volumetric flow rates of the anolyte and catholyte, respectively.

$$\text{PE} = (L - S)/L \tag{9}$$

$$L = \frac{Q_a \cdot c_{anode\ output}}{2(Q_a + Q_c)} = \frac{Q_c \cdot c_{cathode\ output}}{2(Q_a + Q_c)} \tag{10}$$

To synthesize $Ca(OH)_2$ from cell outputs, we first dissolved $CaCO_3$ by adding acidic electrolyte from the cell until no solids were visible and the pH had reached ~3. We then added an equimolar quantity of basic electrolyte to the calcium solution to precipitate $Ca(OH)_2$, which was isolated by filtration. The dry solid was taken for thermogravimetric analysis (TGA) to quantitatively determine the water, carbonate, and residual salt content (Figure 3A). Powder x-ray diffraction (pXRD) showed no peaks from $CaCO_3$ or KCl, and ICP-MS revealed that the dry product contains only 0.15 mol% potassium, indicating a very high purity (> 99%, dry basis) (Figure 3B). Using a combination of real cell outputs and mock solutions of HCl and KOH in KCl (each with a total K^+ concentration of 3 M), we evaluated PE as a function of c_{output} and fit the results to Equation 9 to calculate S, which was found to be 23.2 ± 0.6 mM across our precipitation trials (Figure 3C and Figure S1). The solubility of $Ca(OH)_2$ in pure water under these conditions is 20 – 22.5 mM.[22,23] The slightly higher value of S obtained from our experiments is likely a consequence of the high ionic strength of the electrolyte, which reduces the Ca^{2+} and OH^- activity coefficients.

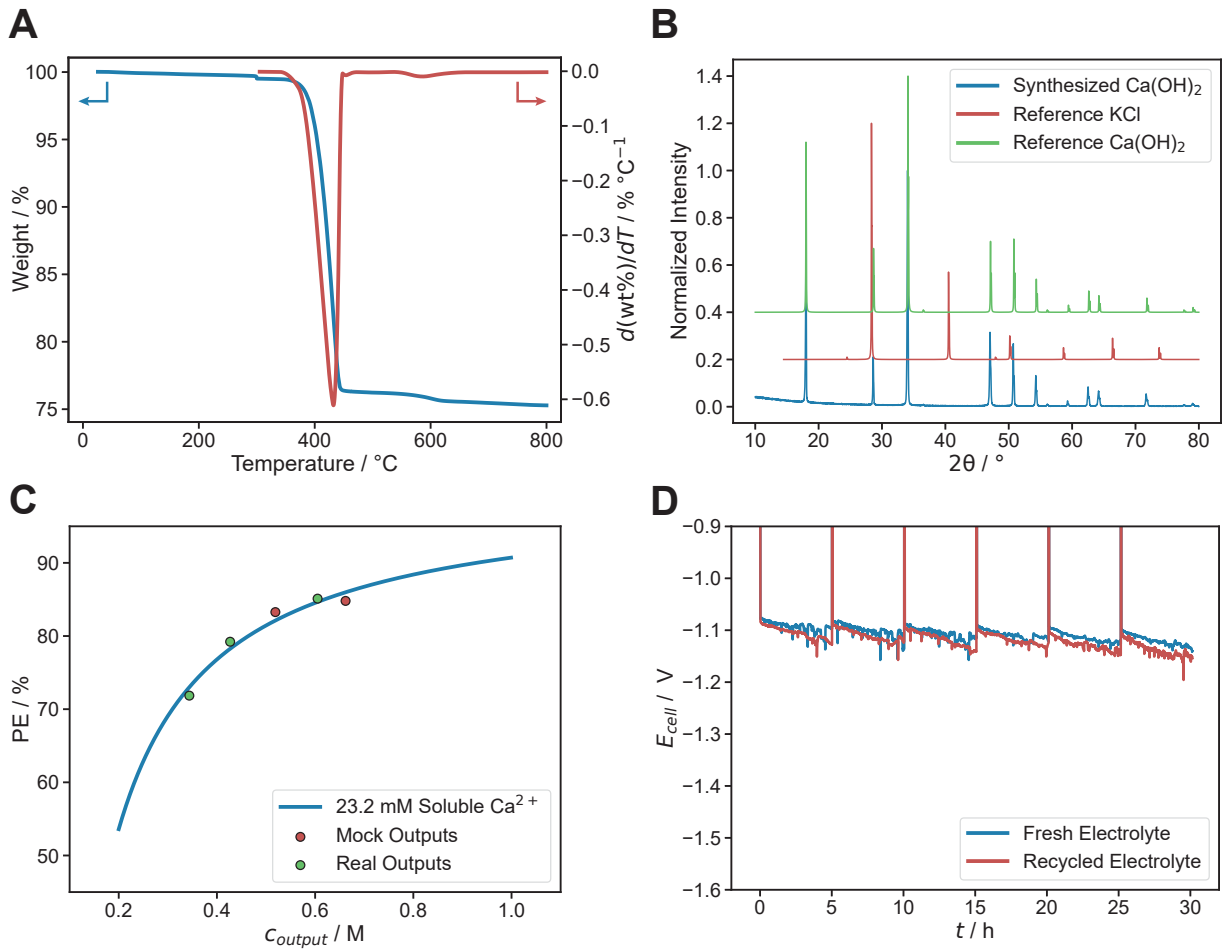

Figure 3: A) Thermogravimetric analysis of $Ca(OH)_2$ product. B) Powder x-ray diffraction $Ca(OH)_2$ product with reference diffractograms for $Ca(OH)_2$ and KCl. C) Precipitation efficiencies for $Ca(OH)_2$ precipitated from DFC outputs or mock solutions of outputs as a function of the concentration of the acid and base streams. D) 30 h operation of the DFC with fresh and recycled 3 M KCl electrolyte at 200 mA cm^{-2} and 50 °C with a $j_{tot}(QF)^{-1}$ ratio of 0.83 M.

To recycle the electrolyte containing residual $Ca(OH)_2$, we slowly bubbled in CO_2 until the pH reached 10 – 10.5 and filtered again to reclaim $CaCO_3$. At this stage, the residual Ca^{2+} concentration could not be reduced below 700 μM (Figure S2). We tested how the residual Ca^{2+} affects cell stability at 50 °C by running the cell at 200 mA cm^{-2} at $j_{tot}(QF)^{-1}$ = 0.83 M. The cell is operated with a 99.7% duty cycle, with brief reverse polarizations at 100 mA cm^{-2} to manage the performance of the commercial gas diffusion electrodes and briefly acidify the cathode to dissolve any precipitates, as previously described.[19,21] While using 3 M KCl as the electrolyte, we observed highly similar average E_{cell} and voltage decay rates between freshly prepared and recycled electrolyte containing residual Ca^{2+} (Figure 3D), with both decay rates < 1 mV h^{-1}.

The isolation of high-purity $Ca(OH)_2$ with the measurement of PE using real cell outputs and the demonstration of electrolyte recycling validates our approach to $Ca(OH)_2$ synthesis and enables a high-level calculation of the overall energy demand for electrochemical $Ca(OH)_2$ production using the DFC. The energy per mol $Ca(OH)_2$ ($E_{Ca(OH)_2}$) is the energy required for 2 moles of acid-base generation divided by the PE for precipitating $Ca(OH)_2$ using the acid and base, as shown in Equation 11.

$$E_{Ca(OH)_2} = \frac{2E_{ab}}{PE} = \frac{2E_{cell}F}{CE \cdot PE} \tag{11}$$

Using the measured CE and E_{cell} values in Figure 2A–D and an S of 23.2 mM as determined above, we calculated $E_{Ca(OH)_2}$ for both electrolytes as a function of j_{prod} at various $j_{tot}(QF)^{-1}$ ratios (Figure 4). For $j_{prod} > 100$ mA cm^{-2}, the intermediate $j_{tot}(QF)^{-1}$ ratio = 0.83 M minimized $E_{Ca(OH)_2}$ by balancing CE losses in the cell with PE losses in precipitation. This trend is reversed at low current density where diffusive CE losses are larger, lowering c_{output} and compounding with PE losses. The contribution of these losses to the total energy efficiency is shown in Figure S3.

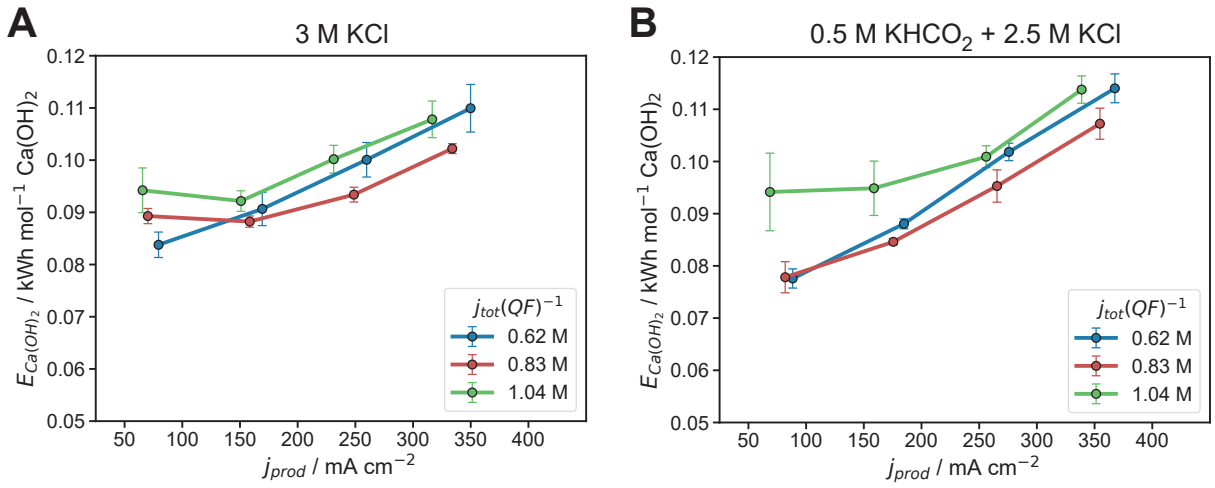

Figure 4: Energy demand for $Ca(OH)_2$ synthesis using the DFC at 50 °C. Energy required per mole to synthesize and precipitate $Ca(OH)_2$ ($E_{Ca(OH)_2}$) vs. j_{prod} at various $j_{tot}(QF)^{-1}$ ratios for A) 3 M KCl and B) 0.5 M $KHCO_2$ + 2.5 M KCl. $E_{Ca(OH)_2}$ is calculated using Equation 11 with PE calculated using Equation 9 assuming S equal to 23.2 mM. Error bars represent the standard deviation of at least 3 independent samples.

The performance of the DFC represents a marked improvement over other cell types (see Table S2). As a point of comparison, concentrated acid and base can be generated at j_{tot} = 20 – 80 mA cm^{-2} by commercial BPMED stacks, and these outputs could be used to drive $Ca(OH)_2$ synthesis. A recent report of a BPMED pilot project produced 1.0 M outputs at an average energy demand of E_{ab} = 0.10 kWh mol^{-1} and a j_{prod} of just 28 mA

cm^{-2} across different operation modes.[24] Considering loss to solubility (assuming S = 20.0 mM $Ca(OH)_2$), a PE of 92% could be achieved for $Ca(OH)_2$ using these outputs, yielding a total energy demand of $E_{Ca(OH)_2}$ = 0.22 kWh mol^{-1} $Ca(OH)_2$ or about 3000 kWh t^{-1}. The DFC requires 60% less energy while operating at 5.6 times the productive rate with 3 M KCl electrolyte (Figure 5A).

Other recently described electrochemical $Ca(OH)_2$ systems report nominally lower energy demand than this estimate for BPMED, but face substantial challenges to achieving steady-state operation. An energy demand of just over 0.16 kWh mol^{-1} was reported for a 3-compartment cell that intentionally accumulates $Ca(OH)_2$ precipitate in the center compartment, but the voltage decay rate exceeded 100 mV h^{-1}, rapidly deteriorating during testing at 200 mA cm^{-2} and necessitating mechanical cleaning of the membranes multiple times per day to recover cell potential.[10] A very low energy demand of 0.057 kWh mol^{-1} was reported for another design featuring a 2-compartment cell that dissolves $CaCO_3$ in the anode chamber and uses an anthraquinone-based redox couple. However, this cell also exhibited a voltage decay rate > 100 mV h^{-1}, partially due to decomposition of the anthraquinone.[14] The relative simplicity of the DFC system reported here is advantageous for advancing toward practical application.

For the purpose of decarbonizing $Ca(OH)_2$, it is important to compare electrochemical approaches to an alternative in which the conventional thermal process is modified to include emissions capture. To estimate the energy demand for avoiding emissions from conventional $Ca(OH)_2$ production, we consider only the lime kiln because CaO hydration is spontaneous and exothermic. The CO_2 in the emissions from the kiln must be upgraded to > 95% and contain less than ~40 ppmv O_2 to prevent corrosion of CO_2 transport pipelines.[25] For the sake of simplicity, we ignore the management of NO_x, SO_x, and CO emissions. The CO_2 can be captured from the kiln exhaust using an amine-based capture plant.[26] We assume that the sorbent is regenerated by a boiler burning natural gas, which adds a modest amount of additional emissions (see Supporting Information), and that the CO_2 is pressurized to 150 bar for pipeline injection. Altogether, the total energy for producing $Ca(OH)_2$ with conventional technology and using carbon capture and sequestration to eliminate the CO_2 emissions is estimated to be 1570 kWh t^{-1} $Ca(OH)_2$. By contrast, the electrochemical approach generates CO_2 without contamination by combustion products, which requires only drying and compression. Assuming carbon-free electricity and the performance metrics demonstrated here, the total energy to produce $Ca(OH)_2$ and pipeline-grade CO_2 using the DFC electrochemical process operating at 200 mA cm^{-2} is just 78% the energy of the thermal process and produces 34% less CO_2 (Figure 5B).[5,27]

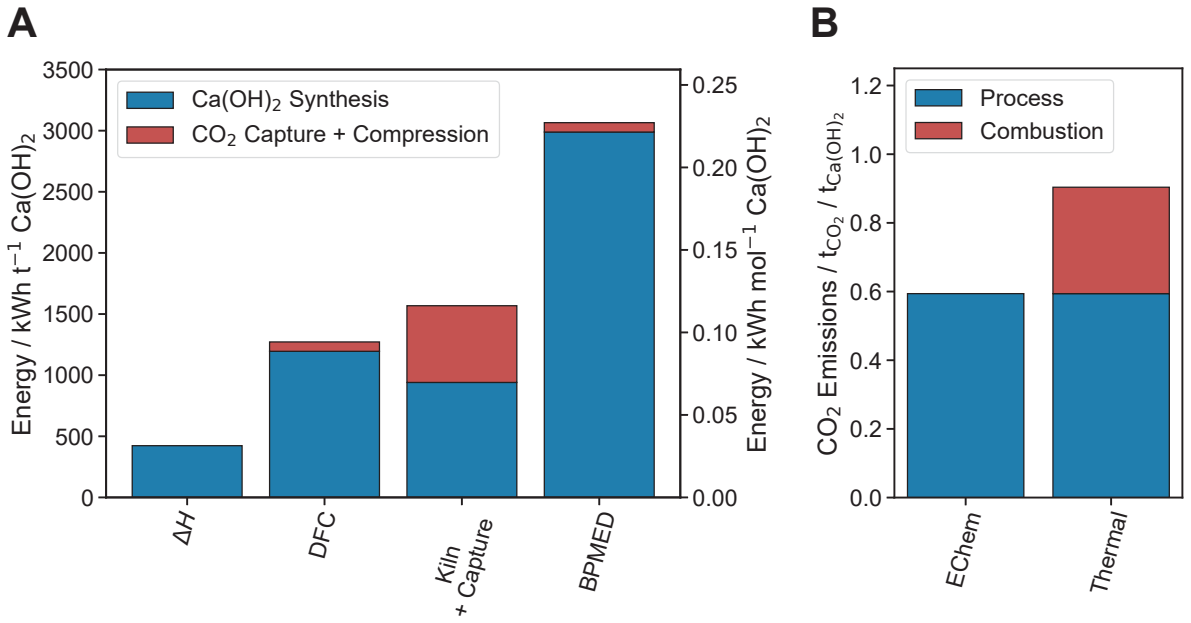

Figure 5: Energy requirements and B) Emissions intensity for producing $Ca(OH)_2$ and pipeline grade CO_2 from $CaCO_3$ and H_2O by various methods.

The data presented in this work demonstrate a streamlined process for the electrification of $Ca(OH)_2$ production. Acid and base chemistry are driven by the DFC, which was demonstrated to produce optimally concentrated outputs at 50 °C with productive current densities up to 334 mA cm^{-2} with 3 M KCl electrolyte and 355 mA cm^{-2} with 0.5 M $KHCO_2$ + 2.5 M KCl mixed electrolyte. At j_{tot} = 200 mA cm^{-2}, the total energy demand for slaked lime production was found to be 0.088 and 0.085 kWh mol^{-1} in these electrolytes, respectively, at an optimal $j_{tot}(QF)^{-1}$ ratio, which represents a marked improvement over what is possible with the established performance metrics of a commercial BPMED stack. In contrast to previous literature on electrochemical slaked lime synthesis, our process does not result in a high voltage decay rate (> 100 mV h^{-1}). Crucially, this process achieved high precipitation efficiencies of > 80% while isolating > 99% purity $Ca(OH)_2$. We compared a decarbonized slaked lime process using the DFC to the incumbent thermal process with carbon capture, finding that electrochemical slaked lime synthesis can offer reduced energy demand as well as reduced emissions. Ongoing work seeks to validate and improve the process with larger scale electrochemical systems.

Acknowledgments

Part of this work was performed at the Stanford Nano Shared Facilities (SNSF) RRID:SCR_023230, supported by the National Science Foundation under award ECCS-2026822. The authors

acknowledge the use of facilities and technical assistance of the Stanford Doerr School of Sustainability Environmental Measurements Facility (RRID: SCR_023255). Dr. Guangchao Li contributed to the collection of ICP-OES and ICP-MS data. Support for this research was provided by the Tides Foundation and the Canadian Institute for Advanced Research. J.G.W. gratefully acknowledges a Stanford Graduate Fellowship. J.W.M is supported by a NSF Graduate Fellowship.

References

(1) U.S. Geological Survey *Mineral Commodity Summaries 2026*.

(2) Kenny, M.; Oates, T. In *Ullmann's Encyclopedia of Industrial Chemistry*; John Wiley & Sons, Ltd: 2007.

(3) Muir, B. M.; Lima, I.; Chudasama, A.; Schiweck, H.; Clarke, M.; Pollach, G. In *Ullmann's Encyclopedia of Industrial Chemistry*; John Wiley & Sons, Ltd: 2025, pp 35–42.

(4) Ecofys *A Competitive and Efficient Lime Industry: Cornerstone for a Sustainable Europe*; Brussels, Belgium: European Lime Association, 2013.

(5) Keith, D. W.; Holmes, G.; St. Angelo, D.; Heidel, K. A Process for Capturing CO2 from the Atmosphere. *Joule* **2018**, *2*, 1573–1594.

(6) Abanades, J. C.; Criado, Y. A.; White, H. I. Direct Capture of Carbon Dioxide from the Atmosphere Using Bricks of Calcium Hydroxide. *Cell Reports Physical Science* **2023**, *4*, DOI: 10.1016/j.xcrp.2023.101339.

(7) Caserini, S.; Storni, N.; Grosso, M. The Availability of Limestone and Other Raw Materials for Ocean Alkalinity Enhancement. *Global Biogeochemical Cycles* **2022**, *36*, e2021GB007246.

(8) Ellis, L. D.; Badel, A. F.; Chiang, M. L.; Park, R. J.-Y.; Chiang, Y.-M. Toward Electrochemical Synthesis of Cement—An Electrolyzer-Based Process for Decarbonating CaCO3 While Producing Useful Gas Streams. *Proceedings of the National Academy of Sciences* **2020**, *117*, 12584–12591.

(9) Zhang, Z.; Mowbray, B. A. W.; Parkyn, C. T. E.; Chris T. E. Waizenegger; Williams, A. S. R.; Lees, E. W.; Ren, S.; Kim, Y.; Jansonius, R. P.; Berlinguette, C. P. Cement Clinker Precursor Production in an Electrolyser. *Energy & Environmental Science* **2022**, 10.1039.D2EE02349K.

(10) Miao, R. K. et al. Electrified Cement Production via Anion-Mediated Electrochemical Calcium Extraction. *ACS Energy Letters* **2023**, *8*, 4694–4701.

(11) Xie, Q.; Wan, L.; Zhang, Z.; Luo, J. Electrochemical Transformation of Limestone into Calcium Hydroxide and Valuable Carbonaceous Products for Decarbonizing Cement Production. *iScience* **2023**, *26*, DOI: 10.1016/j.isci.2023.106015.

(12) Martínez, N. P.; Troncoso P, F.; Gazzano, V.; Ramírez-Amaya, D.; González, M.; Navarrete, I.; Canales, R.; Dreyse, P. High-Performance and Low-Cost Electrochemical Reactor for Limestone Decarbonation Applied to Clinker Production – A Validation at Laboratory Scale. *Journal of Cleaner Production* **2024**, *468*, 143112.

(13) Zhang, Z.; Williams, A. S. R.; Ren, S.; Mowbray, B. A. W.; Parkyn, C. T. E.; Kim, Y.; Ji, T.; Berlinguette, C. P. Electrolytic Cement Clinker Precursor Production Sustained through Orthogonalization of Ion Vectors. *Energy & Environmental Science* **2025**, *18*, 2395–2404.

(14) Ji, T.; Ren, S.; Jiang, G.; Yang, Y.; Ma, S.; Waizenegger, C. E. B.; Kim, Y.; Jewlal, A. M. L.; Stolar, M.; Berlinguette, C. P. Limestone Conversion to Cement Clinker Precursor in a Zero-Gap Electrolyzer. *Journal of the American Chemical Society* **2025**, *147*, 27314–27322.

(15) Ji, T.; Ren, S.; Yang, Y.; Jiang, G.; Crescenzo, G. V.; Scott, S. S.; Kim, Y.; Williams, A. S. R.; Rumscheidt, J.; Stolar, M.; Berlinguette, C. P. Low-Emission Cement Clinker Precursor Production, Enabled by Electrolytic Extraction of Calcium from Waste Cement. *Nature Communications* **2025**, *16*, 9302.

(16) Finke, C.; Dry, M. J.; Kashyap, V.; Karumb, E. T.; Harvey-Costello, N.; Bresson, J. A.; Keller, M. J.; Leandri, H. F. (Brimstone Energy Inc). Cementitious Material Production from Non-Limestone Material US Patent, 11964922B2, 2024.

(17) Benck, J. D.; Chiang, Y.-M.; Ellis, L. D.; Dominguez, K.; Layurova, M. (Sublime Systems Inc). Electrochemical Materials Production and Processing US Patent, 12187647B2, 2025.

(18) Justnes, H. Alternative Low-CO2 "Green" Clinkering Processes. *Reviews in Mineralogy and Geochemistry* **2012**, *74*, 83–99.

(19) Charnay, B. P.; Chen, Y.; Misleh, J. W.; Wright, J. G.; Agarwal, R. G.; Sauvé, E. R.; Toh, W. L.; Surendranath, Y.; Kanan, M. W. Membrane-Free Electrochemical Production of Acid and Base Solutions Capable of Processing Ultramafic Rocks. *Nature Communications* **2025**, *16*, 9759.

(20) Wright, J. G.; Kanan, M. W. Electrochemical Production of >1 M Acid and Base from Neutral Salt at High Current Density and Low Energy Demand. *ACS Energy Letters* **2025**, *10*, 5328–5335.

(21) Misleh, J. W.; Wright, J. G.; Charnay, B. P.; Kanan, M. W. Li-Ion Battery Recycling by Energy-Efficient, High-Throughput Li2SO4 Salt Splitting in a Diaphragm Flow Cell. *Watt* **2026**, *1*, 4.

(22) Kutus, B.; Gácsi, A.; Pallagi, A.; Pálinkó, I.; Peintler, G.; Sipos, P. A Comprehensive Study on the Dominant Formation of the Dissolved Ca(OH)2(Aq) in Strongly Alkaline Solutions Saturated by Ca(II). *RSC Advances* **2016**, *6*, 45231–45240.

(23) Castaño, S. V.; La Plante, E. C.; Collin, M.; Sant, G.; Pilon, L. A Pilot-Process for Calcium Hydroxide Production from Iron Slag by Low-Temperature Precipitation. *Journal of Environmental Chemical Engineering* **2022**, *10*, 107792.

(24) Cassaro, C.; Virruso, G.; Culcasi, A.; Cipollina, A.; Tamburini, A.; Micale, G. Electrodialysis with Bipolar Membranes for the Sustainable Production of Chemicals from Seawater Brines at Pilot Plant Scale. *ACS Sustainable Chemistry & Engineering* **2023**, *11*, 2989–3000.

(25) Shirley, P.; Myles, P. *Quality Guidelines for Energy System Studies: CO2 Impurity Design Parameters*; NETL-PUB–22529; National Energy Technology Laboratory (NETL), Pittsburgh, PA, Morgantown, WV, and Albany, OR (United States), 2019.

(26) Simoni, M.; Wilkes, M. D.; Brown, S.; Provis, J. L.; Kinoshita, H.; Hanein, T. Decarbonising the Lime Industry: State-of-the-art. *Renewable and Sustainable Energy Reviews* **2022**, *168*, 112765.

(27) Boot-Handford, M. E. et al. Carbon Capture and Storage Update. *Energy & Environmental Science* **2013**, *7*, 130–189.